Excited state properties of donor bound excitons in ZnO

Bruno K. Meyer,* Joachim Sann, Sebastian Eisermann, and Stefan Lautenschlaeger
I. Physics Institute, Justus-Liebig University, Heinrich-Buff-Ring 16, 35592 Giessen, Germany

Markus R. Wagner, Martin Kaiser, Gordon Callsen, Juan S. Reparaz, and Axel Hoffmann
Institute of Solid State Physics, Technical University Berlin, Hardenbergstr. 36, 10623 Berlin, Germany
(Received 30 July 2010; published 14 September 2010)

ZnO shows a great variety of richly structured luminescence lines in a very narrow energy range of 30 meV below the free *A*-exciton line. At very low temperatures the majority of these lines can be explained by radiative recombination of excitons bound to neutral and ionized donors. With increasing temperature even more photoluminescence (PL) lines appear with activation energies which indicate the involvement of excited states of the bound exciton complexes. Based on high-resolution temperature-dependent luminescence and luminescence excitation experiments we investigate the excited states properties of donor bound excitons in ZnO. Several possible configurations of excited states could be distinguished: (i) excitons which involve a hole from the *B*- instead of the *A*-valence band, (ii) vibrational-rotational excited states of the excitons, and (iii) electronic excited states of the excitons. Magneto-PL measurements of the ground and vibrational-rotational excited states corroborate the identification of the excited states with comparable *g*-factors for all shallow donor bound excitons. In addition to the excited states, energy transfer processes via the ionized bound excitons and free exciton polaritons are observed. The experimental results are supported by theoretical calculations and demonstrate that ZnO is a unique compound semiconductor where the basics of atomic and molecular physics can be studied and understood in a solid state matrix.

DOI: 10.1103/PhysRevB.82.115207 PACS number(s): 71.10.Li, 71.35.−y, 71.55.Gs, 78.55.Et

I. INTRODUCTION

The possibility to dope ZnO *p*-type and thus allow for the realization of optoelectronic devices has been in the focus of interest in recent years for ZnO and its alloys MgZnO and CdZnO.[1] The incorporation of electrically active shallow acceptors can best be monitored by the respective changes in the near band edge radiative recombinations. It requires, however, knowledge about the structure of the bound exciton complexes, present in as-grown nominally undoped ZnO. Recently, we reported on the trends in the localization energies of neutral (D^0X) and ionized (D^+X) donor bound excitons,[2,3] where the structure of the bound excitons has been verified by extensive magneto-optical experiments. These investigations focused on the prominent D^0X recombination lines (I_4, I_6, I_8, and I_9) and their D^+X counterparts. However, in high quality homoepitaxial films and bulk crystals many more lines can be observed and new lines appear at higher temperatures.[4] By using temperature-dependent photoluminescence (PL) and photoluminescence excitation (PLE) spectroscopy we were able to divide the recombination lines in two classes: (i) bound excitons in the ground state where the hole of the exciton comes from the *A*-valence band (D^0X_A,D^+X_A) and (ii) bound excitons excited states. On an energy scale—as we will show—the latter class can be further divided into three subclasses: rotational-vibrational states of the bound exciton complexes, donor bound excitons where the *A*-valence band hole is replaced by a hole from the *B*-valence band (i.e., D^0X_B), and electronic excited states of the excitons (see the schematic of Fig. 1).

Blattner *et al.*[5] and Gutowski *et al.*[6] reported earlier on photoluminescence excitation spectra of the various bound excitons. Groups of resonances were observed and explained by rotational or vibrational excited states of the bound excitons and states where the *B*-valence band is involved. For a compilation of older data including excitation spectra in the presence of magnetic field we refer to Ref. 5 (see Figs. 5 and 7 therein). Blattner *et al.*[5] found excited states for I_9 and I_{10} with an energy 9 meV above the ground state which is two times the *A*-*B* valence band splitting (2×4.5 meV). These lines were assigned to A^0X states involving two holes from the *B*-valence band. Emission lines which are generally assigned to D^0X did not show this excitation level. Gutowski *et al.*[6] performed intensity dependent high-resolution excitation spectroscopy and assigned most of the observed emission bands (I_5 to I_{11}) to A^0X states, an interpretation which does

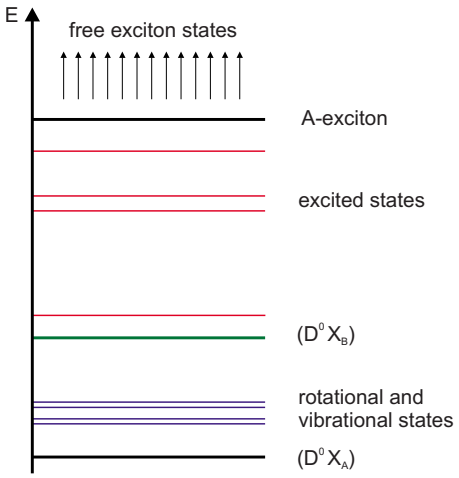

FIG. 1. (Color online) Schematic of bound exciton ground and excited state recombinations observed in ZnO (energies are not to scale).

no longer hold in the light of recent magneto-optical and PL experiments.[3,7,8]

In this work we will show that temperature-dependent steady-state excitation measurements of high-quality ZnO bulk crystals are sufficient to resolve most of the spectral details of the excited states of the bound excitons. The experiments are extended to luminescence excitation and magneto-PL measurements and compared to theoretical calculations which enable a comprehensive study of donor excited state properties and energy-transfer mechanisms in ZnO.

II. EXPERIMENTAL DETAILS

For the temperature-dependent PL measurements bulk crystals from Cermet Inc. grown by the pressurized melt growth technique were employed, which exhibited numerous transition lines with linewidths as small as 140 μeV. In addition to the Cermet crystals, bulk crystals from Tokyo Denpa and MTI Corp. as well as nominally undoped homoepitaxial films grown by CVD on ZnO substrates from CrysTec were studied. Naturally, different donor concentrations in the samples lead to varying intensities of the specific bound excitons which also affected the observability of the excited states in the photoluminescence spectra. However, comparable results of different samples proofed that the experimentally and theoretically derived excited state properties of donor bound excitons are valid for all investigated ZnO samples.

Excitation was performed by the 325 nm line of a HeCd laser and the luminescence was dispersed by a 1 m Jobin Yvon monochromator equipped with a Hamamatsu R375 photomultiplier. Magneto-PL spectra were recorded in a 5 T split-coil magnetocryostat. The PLE spectra were recorded using a dye laser containing 2-methyl-5-t-butyl-p-quaterphenyl which was pumped by the 308 nm line of a XeCl excimer laser. The excitation wavelength was tuned in the range from 345 to 375 nm. The laser was operated in pulsed mode with a repetition rate of 100 Hz and a quasi-cw power of 10 mW. The spectral resolution of the setup was better than 0.1 Å.

III. EXPERIMENTAL RESULTS

A typical photoluminescence spectrum recorded at 10 K is shown in Fig. 2. The lines are labeled from 0 to 9 with additional indices. For an assignment of these lines see Table I. At T=4.2 K fewer lines are observed (not shown) which indicates that some of the transitions originate from ground states and others from excited states. A_T and A_L mark the position of the free A-exciton (T: transversal, L: longitudinal) energies. For the D^0X_A and D^+X_A recombinations, respectively, the energetic distance to the A_T line position is called localization energy.

Detailed temperature-dependent measurements showed that the recombination lines can be divided into two groups: (i) recombination lines which rapidly loose intensity with increasing temperature and (ii) lines whose intensity first increases with increasing temperature before they start to loose

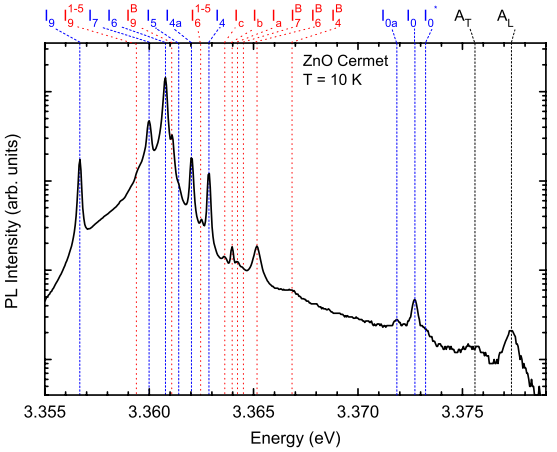

FIG. 2. (Color online) Photoluminescence spectrum of a ZnO single crystal recorded at 10 K. Dashed (blue) lines mark the transitions of neutral and ionized donor bound excitons, dotted (red) lines indicate excited states of donor bound excitons.

intensity. The former group of lines is shown in Fig. 3 exemplified for the two transitions I_{0a} and I_9, which were identified as D^+X and D^0X recombinations, respectively.[3,7,8] They show a thermally activated decrease whereby the activation energies E_1 obtained by fitting to the experimental data are related to the strength of the localization of the excitons at the impurity and correspond to the respective localization energies.

The transitions marked by the dashed (blue) lines in Fig. 2 are related to bound exciton recombination lines, which show only a thermally activated decrease in the luminescence intensity. They belong to the neutral and ionized donor bound exciton transitions, and their character was firmly established by magneto-optical experiments.[3,7,8] In contrast, the recombination lines marked by the dotted (red) lines (e.g., lines I_a to I_c) exhibit a different temperature dependence which can be understood with help of Fig. 4.

TABLE I. Energy positions of free and bound excitons in bulk ZnO crystals. I_i^B denote excitons involving a hole from the B-valence band and I_i^{1-5} mark vibrational-rotational excited states. For a precise differentiation of these states see Table II.

Energy (eV)	Ground-state transition	Energy (eV)	Excited-state transition
3.3773	A_L	3.3669	I_4^B (D^0X_B)
3.3758	A_T	3.3652	I_6^B (D^0X_B)
3.3732	I_0^* (D^+X_A)	3.3645	I_7^B (D^0X_B)
3.3727	I_0 (D^+X_A)	3.3643	I_8^B (D^0X_B)
3.3719	I_{0a} (D^+X_A)	3.3642	I_a
3.3628	I_4 (D^0X_A)	3.3639	I_b
3.3620	I_{4a} (D^0X_A)	3.3636	I_c
3.3614	I_5 (D^0X_A)	3.3624	I_6^{1-5} (D^0X_A)
3.3608	I_6 (D^0X_A)	3.3619	I_7^{1-5} (D^0X_A)
3.3600	I_7 (D^0X_A)	3.3617	I_8^{1-5} (D^0X_A)
3.3598	I_8 (D^0X_A)	3.3611	I_9^B (D^0X_B)
3.3567	I_9 (D^0X_A)	3.3594	I_9^{1-5} (D^0X_A)

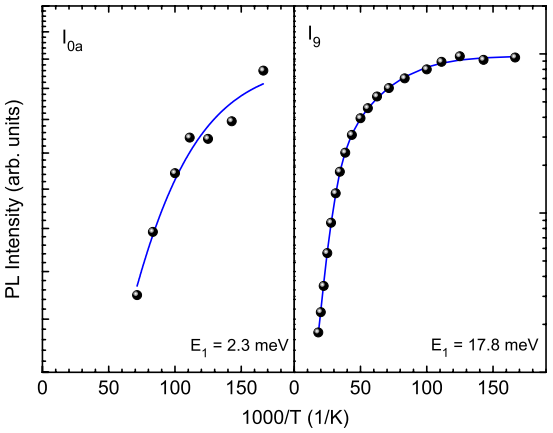

FIG. 3. (Color online) Arrhenius plots of the recombination lines I_{0a} and I_9. Dots are experimental data, solid lines are fits to the data with the resulting activation energies.

An increase in temperature from 4.2 K to approximately 20 K leads to an increase in the luminescence intensity expressed by the activation energy E_a. With a further increase in temperature the intensity decreases, thermally activated with the activation energies E_1 (see Fig. 4). The activation energies E_1 range between 15 and 20 meV and are indicative of the thermal decay of neutral donor bound excitons since E_1 scales with the localization energies. The activation energies E_a range from 2 to 4 meV and indicate that excited states of the exciton are involved. Several scenarios are possible for the configurations of excited states of the exciton bound to a neutral donor leaving the donor in the ground state (excited states of the donor leaving the exciton in the ground state are known as the TES transitions, see Ref. 9) (i) excitons which involve a hole from the *B*- instead of the *A*-valence band, (ii) vibrational-rotational excited states of the excitons, and (iii) electronic excited states of the excitons.

Recombination lines which belong to class (i) can be identified on the basis of their line separations from the respective D^0X_A transitions which should be in close agreement with the energetic distance between the *A*- and

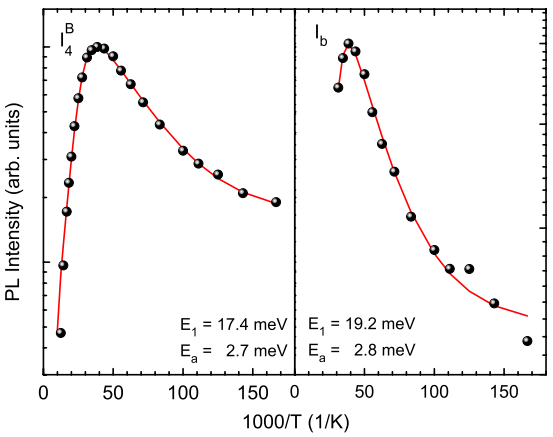

FIG. 4. (Color online) Arrhenius plots of the recombination lines I_4^B and I_b. Dots are experimental data, solid lines are fits to the data with the resulting activation energies.

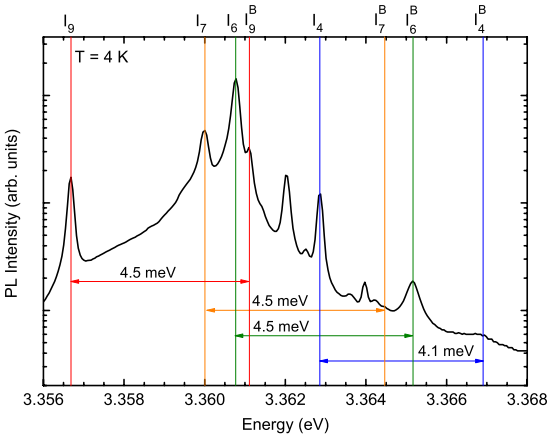

FIG. 5. (Color online) Photoluminescence spectrum of a ZnO single crystal recorded at 10 K. Vertical drop lines mark recombinations of neutral donor bound excitons with holes from the *A*- and *B*-valence band.

B-valence bands. As shown in Fig. 5, I_9, I_7, and I_6 have matching lines which are placed 4.5 meV higher in energy (the spacing between the *A*- and *B*-valence bands is 4.7 meV). For I_4 the distance is slightly smaller, but the high energy line tentatively identified with I_4^B is significantly broader compared to I_6^B or I_7^B. The activation energies E_a of 2.5–4 meV obtained from the temperature-dependent PL of the bound exciton states with *B*-valence band holes are in fair agreement with the size of the *A*-*B* splitting. The remaining lines (I_a to I_c and I_6^{1-5}) can be attributed to process (ii)—vibrational-rotational excited states of the excitons as will be substantiated below. Before we present the corresponding calculations it is interesting to compare the findings with the results obtained by luminescence excitation spectroscopy where even more details can be resolved.

In the PLE experiments the intensity of a specific bound exciton transition is monitored while the excitation light is tuned to higher energies. Thereby we cannot only observe the details of the bound exciton excited states but also transfer processes via the exciton (polariton) ground and excited states. This is shown in Fig. 7 for the case of I_6. Up to the position of the free *A*-exciton $[A_L(\Gamma_5)]$ various bound exciton excited states show up, for higher energies the ground and excited states of the free *A*, *B*, and *C* excitons contribute to the energy transfer. The top axis of Fig. 7 denotes the energy spacing from the I_6 line between 0 and 16 meV. At 4.5 meV above I_6 the contribution of an excited state related to the *B*-valence band is clearly visible. The terms I_6^{1-5} and I_6^{a-e} will be explained on the basis of the following calculations.

IV. INTERPRETATION OF THE EXCITED STATE TERMS

A preliminary estimate of the vibrational-rotational states of a neutral donor bound exciton was given in Ref. 9. We have extended theses calculations to include also electronic excited states of the exciton and derived the following results: an estimate of the vibration and rotation energies of the bound excitons can be obtained if the analogy to molecular

TABLE II. Calculated vibrational-rotational energies for different quantum numbers ν and J of the donor bound excitons I_9, I_8, I_7, I_6, and I_4 with D being the localization energy of the bound exciton and $E(0,0)$ the energy according to Eq. (2) with $\nu=0$ and $J=0$. The experimental values are determined from the PL and PLE spectra in Figs. 6 and 7.

								Energy above ground state	
Exciton	Energy (eV)	D (meV)	$E(0,0)$ (meV)	Excited state	ν	J	Excited state energy (eV)	Theory (meV)	Experiment (meV)
I_9	3.3567	19.1	3.06	I_9^1	0	1	3.35874	2.04	2.0 (PLE)
				I_9^2	1	0	3.35884	2.14	2.0 (PLE)
				I_9^3	0	2	3.35927	2.57	2.65
				I_9^4	1	1	3.35928	2.58	2.65
				I_9^5	2	0	3.35931	2.61	2.65
I_8	3.3598	16.0	2.25	I_8^1	0	1	3.36132	1.52	
				I_8^2	1	0	3.36138	1.58	
				I_8^3	0	2	3.36170	1.90	1.94
				I_8^4	1	1	3.36171	1.91	1.94
				I_8^5	2	0	3.36173	1.93	1.94
I_7	3.3600	15.8	2.20	I_7^1	0	1	3.36149	1.49	
				I_7^2	1	0	3.36155	1.55	
				I_7^3	0	2	3.36186	1.86	1.88
				I_7^4	1	1	3.36187	1.87	1.88
				I_7^5	2	0	3.36189	1.89	1.88
I_6	3.3608	15.0	2.01	I_6^1	0	1	3.36212	1.32	1.4 (PLE)
				I_6^2	1	0	3.36217	1.37	1.4 (PLE)
				I_6^3	0	2	3.36244	1.64	1.67
				I_6^4	1	1	3.36245	1.65	1.67
				I_6^5	2	0	3.36246	1.66	1.67
I_4	3.3628	13.0	1.56	I_4^1	0	1	3.36386	1.06	
				I_4^2	1	0	3.36389	1.09	
				I_4^3	0	2	3.36411	1.31	
				I_4^4	1	1	3.36411	1.31	
				I_4^5	2	0	3.36412	1.32	

vibrations is considered. Using a Kratzer potential

$$V(r) = -2D\left(\frac{a}{r} - \frac{a^2}{2r^2}\right) \tag{1}$$

leads to

$$E(\nu,J) = -\frac{(2ma^2/\hbar^2)D^2}{\left[\left(\nu+\frac{1}{2}\right) + \sqrt{\left(J+\frac{1}{2}\right)^2 + \left(\frac{2ma^2}{\hbar^2}\right)D}\right]^2}, \tag{2}$$

where ν and J are the vibrational and rotational quantum numbers, respectively. D is the binding (or localization) energy of the bound exciton, m is the relevant band mass and a the distance electron (hole) impurity. The donor bound excitons are described in analogy to the "pseudodonor model" for acceptor bound excitons. In this model, the hole of the exciton is tightly bound to the neutral acceptor and the electron is in a large orbit around the positive core. In such a case the band mass for electrons would enter into Eq. (2) as well as a distance of 1.8 nm (Bohr radius). For donor bound excitons, we assume that the electron is tightly bound and the hole is in a large orbit. With a band mass of $m=0.7m_0$ which is calculated from the acceptor ionization energy of 165 meV by using the simple effective mass theory (EMT) approach, a distance of $a=0.8$ nm results. The energy above ground state is then calculated as the difference between $E(0,0)$ and $E(\nu,J)$.

The excited state levels are calculated for $\nu=0$, 1, and 2, and $J=0$, 1, and 2 for the neutral donor bound excitons I_4, I_6, I_7, I_8, and I_9. Evidently, there is a remarkably good agreement between the calculated and the experimental results with this rather simple model (see Table II). Experimentally it is not always possible to distinguish between vibrational and rotational states since they are very close in energy and partially overlap. The excited states are grouped into two main transitions which are separated by only 0.2–0.6 meV (see Table II). In the temperature-dependent PL measurements mainly vibrational-rotational excited states (apart from D^0X_B) have been observed. These are, in particular, the overlapping excited states of the strongest bound exciton I_6 (I_6^{1-5}) and the transitions labeled I_a to I_c. The I_6^{1-5} states are also

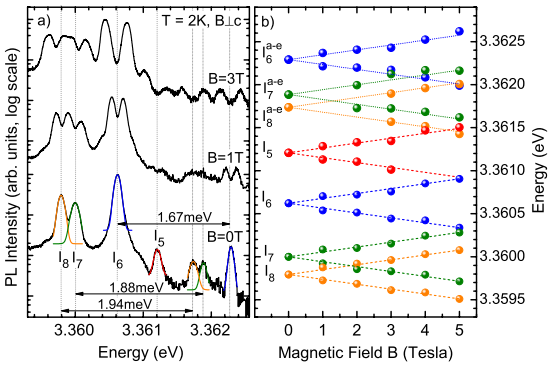

FIG. 6. (Color online) (a) Magneto-PL spectra of a homoepitaxial ZnO film recorded at 2 K at field strengths of 0, 1, and 3 T in the Voigt configuration ($\boldsymbol{B} \perp \boldsymbol{c}$). Vibrational-rotational excited states are observed for the bound excitons I_8, I_7, and I_6. (b) Peak energies of the Zeeman split transition lines for ground and excited states as function of the magnetic field strength between 0 and 5 T.

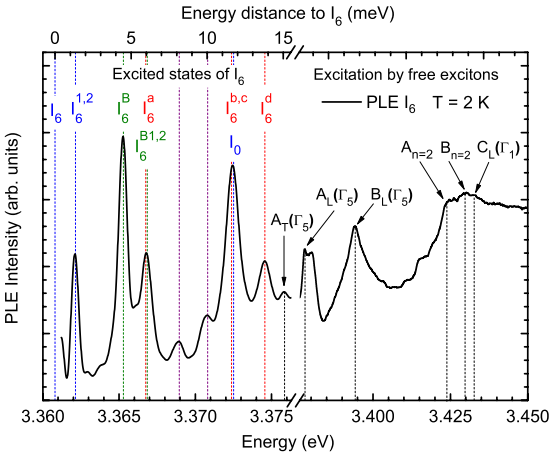

FIG. 7. (Color online) Luminescence excitation spectrum monitored at the I_6 recombination line. Excitation channels exist via the free (A, B, and C) exciton polaritons and their excited states ($n=2$) and for the neutral donor bound exciton excited states (note the change in the energy scale). The energy spacing of the excitation channels to the I_6 line is displayed in the top x axis.

observed as excitation channels in the PLE spectrum in Fig. 7 although not completely resolved. Based on their energetic position, the excited states I_a to I_c are tentatively attributed to the I_4 and I_{4a} transitions.

Under the influence of an external magnetic field, the ground and excited states are split by the Zeeman effect according to their electron and hole g-factors. Figure 6(a) shows the magneto-PL spectra of a homoepitaxial grown ZnO film in the Voigt configuration $\boldsymbol{B} \perp \boldsymbol{c}$. At zero field, not only the bound exciton ground-state recombination lines I_6, I_7, and I_8 are observed but also the corresponding vibrational-rotational excited states are visible for all three excitons (Table II). The narrow linewidth of the bound excitons allows a spectral separation of the Zeeman components already at a field strength of 1 Tesla [see Fig. 6(a)]. The peak energies of the split ground and excited state lines are displayed as function of the magnetic field in Fig. 6(b). From the size of the splitting, an electron g value of $g_e^{\perp}=1.96$ is derived for the ground states of all three bound excitons in good agreement with previous magneto-PL studies of shallow bound excitons in ZnO.[3,6,7] Although an additional splitting of the exciton lines caused by a non vanishing hole g-factor $g_h^{\perp}$ is clearly observed for magnetic fields greater than 3 T, this splitting is neglected in the fits of Fig. 6(b) for reasons of clarity and simplicity. A detailed discussion of this Γ_7 valence band symmetry related hole fine splitting in the Voigt configuration was recently published by Wagner *et al.*[7] For the excited states of I_6, I_7, and I_8 a comparable splitting into two Zeeman components is observed in the magneto-PL spectra. The analysis of the peak energies reveals that the splitting of the excited state transition line can be modeled by the same g values as their respective ground-state excitons. The comparable Zeeman splittings of ground state and excited state excitons support the assignment of these line to vibrational-rotational excited states since the same electron and hole states with equal g-factors as in the ground state are involved.

Apart from the vibrational and rotational states, electronic excited states of the exciton exist (process iii) which are obviously much easier resolvable in PLE experiments (see Fig. 7). For the description and calculation of the energy terms we followed a formalism presented by Puls *et al.*[10] for donor-exciton complexes in CdS.

The energy of the excited states of donor bound excitons is given by

$$E = E_G + 2R_D\left[a^2 - \frac{11}{8}a - \frac{s^2t^2}{2}\sigma^{-1} \times \left(n_r + \frac{1}{2} + \sqrt{\left(l+\frac{1}{2}\right)^2 + \frac{st^2}{a}\sigma^{-1}}\right)\right]^{-2}, \quad (3)$$

where E_g is the energy band gap of ZnO, R_D is the effective Rydberg energy of the donor (or the donor binding energy E_D), and $a=a_e/a_D$ is the ratio of the Bohr radii of the electrons in the exciton a_e and the donor a_D, respectively. n_r and l are the orbital (radial) and angular momentum quantum numbers of the exciton, $\sigma=m_e^*/m_h^*$ is the ratio of electron and hole masses. The variables s and t where taken from Puls *et al.*[10] as $s=1.0136$ and $t=1.337$. These values should be valid for exciton-impurity-complexes, in general, i.e., also for ZnO. Equation (3) should be adjusted to ground state positions of the neutral donor bound excitons with $n_r=0$ and $l=0$ for which R_D (i.e., E_D) and the ratio of the Bohr radii were varied to achieve agreement. The excited state levels are calculated for $\nu=0$, 1, and 2, and $J=0$ 0, 1, and 2. The parameters and results of the calculation are given in Table III.

Based on these calculations, four excited states (I_6^{a-d}) observed in the PLE experiments could be assigned to I_6 as shown in Fig. 7. Thereby, the first excited state I_6^a ($n_r=0$, $l=1$) has the same energy as the vibrational-rotational states of the I_6^B exciton ($I_6^{B1,2}$). As expected from the parameters used in the calculation (Table III) the excited state energies are quite similar for I_9 to I_6. With decreasing localization energy, e.g., for I_4 three excited states merge with the free A-exciton line whereas only one is well below the A exciton

TABLE III. Calculated electronic excited state energies for different quantum numbers n_r and l of the donor bound excitons I_9, I_8, I_7, I_6, and I_4 with E_D being the donor binding energy and a the ratio of the Bohr radii. Values in brackets indicate unstable states above the A_T free exciton. The experimental values are determined by PLE measurements.

								Energy above ground state	
Exciton	Energy (eV)	E_D (meV)	a	Excited state	n_r	l	Excited state energy (eV)	Theory (meV)	Experiment (meV)
I_9	3.3567	55.8	0.775	I_9^a	0	1	3.3629	6.2	6.0
				I_9^b	1	0	3.3696	12.9	14.2
				I_9^c	0	2	3.3697	13.0	14.2
				I_9^d	1	1	3.3723	15.6	15.9
				I_9^e	2	0	3.3754	18.7	18.1
I_8	3.3598	53.7	0.775	I_8^a	0	1	3.3658	6.0	
				I_8^b	1	0	3.3721	12.3	
				I_8^c	0	2	3.3722	12.4	
				I_8^d	1	1	3.3747	14.9	
				I_8^e	2	0	(3.3778)	(18.0)	
I_7	3.3600	53.55	0.775	I_7^a	0	1	3.3660	6.0	
				I_7^b	1	0	3.3723	12.3	
				I_7^c	0	2	3.3724	12.4	
				I_7^d	1	1	3.3749	14.9	
				I_7^e	2	0	(3.3779)	(17.9)	
I_6	3.3608	53.0	0.775	I_6^a	0	1	3.3667	5.9	5.9
				I_6^b	1	0	3.3729	12.1	11.5
				I_6^c	0	2	3.3731	12.4	11.7
				I_6^d	1	1	3.3755	14.7	13.9
				I_6^e	2	0	(3.3785)	(17.7)	
I_4	3.3628	51.6	0.775	I_5^a	0	1	3.3686	5.8	
				I_5^b	1	0	3.3747	11.9	
				I_5^c	0	2	3.3748	12.0	
				I_5^d	1	1	(3.3772)	(14.4)	
				I_5^e	2	0	(3.3801)	(17.3)	

($n_r=0$, $l=1$) but falls into the region where the D^+X transitions occur. This explains why it is not easy to observe the electronic excited states in steady state PL measurements, only the selective excitation in PLE enables the enhancement in spectral contrast. The excited states with highest energy in Table III are given for the I_i^e states ($n_r=2$, $l=0$). For all excitons above I_9, the energies of these excited states are greater than the energy of the free exciton A_T. Consequently, the (2,0) excited states are not stable and can only be observed for the I_9 exciton and below. The best fit to the experiment can be achieved for those donors where central cell effects are smallest,[9] i.e., I_4 to I_6. For ZnO, however, polaron contributions to the binding energy of the donors are significant[9] and only 75% of the donor binding energy (in the absence of central cell effects) can be accounted for by a simple EMT approach, where E_D is proportional to m_e^*/ϵ^2. Thus the calculations in spite of the good agreement for I_6 can only be semiquantitative but of considerable help to understand the nature of the electronic excited states.

V. DISCUSSION AND CONCLUSION

Two recent publications[7,8] dealt with the magneto-optical properties of bound exciton emissions. Based on polarization and angular resolved magnetophotoluminescence spectroscopy both works derive the same findings: they confirm the ordering of the valence band (A, B, and C) as a sequence of Γ_7, Γ_9, and Γ_7, and they unambiguously identify charge states of the defect centers and exciton types. I_4, I_5, I_6, I_7, I_8, and I_9 are due to neutral donor bound excitons, while I_0, I_1, I_2, and I_3 are caused by ionized donor bound excitons. For all those recombination lines holes from the A-valence band are involved. For three remaining lines (labeled 5, 7, and 10 in Ref. 8) Ding *et al.*[8] could not provide a conclusive identification but the transitions 5 and 7 could originate from excited states and are very likely vibrational-rotational excited states of I_6 and I_4, respectively. We have used the information from the magneto-optical investigations on the different exciton types to obtain the trends for A- and B-valence band related bound exciton recombinations. These experimental

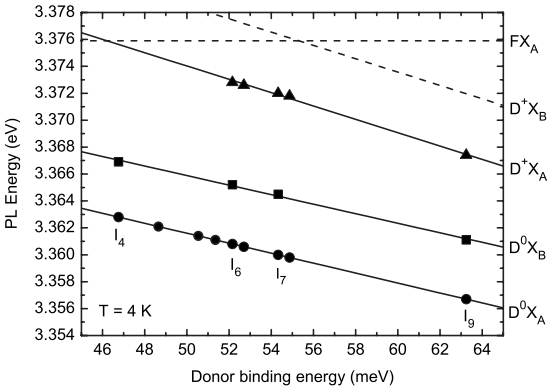

FIG. 8. Energy position as a function of donor binding energy for neutral and ionized donor bound excitons involving *A*- and *B*-valence bands at 4 K.

findings on the neutral and ionized donor bound excitons involving the *A*- and *B*-valence band states are summarized in Fig. 8. The donor binding energies were obtained from the localization energies under assumption of validity of Haynes rule.[9,11] The equal slopes of D^0X_B compared to D^0X_A in Fig. 8 are a consequence of the identical binding energies (and thus identical hole masses) of the *A*- and *B*-valence band related free excitons. The trend for D^+X_B (dashed line in Fig. 8) compared to D^+X_A (Ref. 2) is also based on the assumption of identical hole masses. The D^0X_A transitions shown by circles in Fig. 8 involve neutral shallow donors, but for only four of them (I_4, I_6, I_8, and I_9) we definitely know the chemical origin.[9]

A decisive and unambiguous assignment to a specific impurity for, e.g., I_5 or I_7 cannot be made at present. In general, we can expect that the elements from group III and group VII of the periodic table act as shallow donors. For group III the only remaining candidate would be boron (Al, Ga, and In have been identified[9]) but it is not a typical trace impurity in bulk crystals and epitaxial films. This leaves the halogens F, Cl, Br, and I as prime suspects. Indeed chlorine was identified as a shallow donor in the early electron paramagnetic resonance work of Kasai[12] and there is indirect evidence that I_5 is caused by chlorine. It remains to be investigated why the chemical origin of I_5 and I_7 escaped its detection up to now.

The ordering of the excited states as outlined in Fig. 1 holds for all neutral donor bound excitons and is found for all investigated ZnO bulk crystals and epitaxial films. We find the excitation resonances at unchanged positions and their intensities (superior for Tokyo Denpa compared to MTI which obviously reflects the crystal quality) also independent of the excitation geometry. The vibrational-rotational states are at most 1.0–2.6 meV above the ground state depending on the localization energy (I_4 to I_9), D^0X_B is independent of the localization energy always 4.5 meV higher in energy, and the electronic excited states give rise to four transitions starting at approximately 6 meV up to 16 meV above the ground state.

As seen in Fig. 7, there still remain two transitions (dashed purple lines with an energy of 8.1 and 10.0 meV above the I_6) which cannot be explained by these attributions. Gutowski *et al.*[6] proposed that in the excitation spectrum of a specific exciton line (e.g., I_6) transitions may show up which are related to the creation of more weakly bound excitons in the electronic ground state i.e., I_5 and I_4 and the ionized donor bound excitons I_3 to I_0. However, the remaining lines do not exactly match the energies of known bound excitons in ZnO and we do not find conclusive evidence for energy-transfer processes from higher to lower energy excitons involving different impurity centers. By contrast, charge-transfer processes from ionized to neutral bound excitons bound to the same impurity can occur.[13] In the case of the I_6, the strong excitation peak at around 3.3725 eV might therefore consist of overlapping excitation channels involving the $I_6^{b,c}$ states and the corresponding ionized bound exciton I_0.[13]

Additional fine structure also arises by the anisotropy of the hole mass, which has been neglected in the calculation leading to Eq. (3). The states (n_r=0) with angular momentum l=1 and l=2 are for isotropic mass threefold and fivefold degenerates, respectively. They can further split into a total of five excited states instead of two.[10] Since, however, polaron-coupling effects are also of relevance for the energy positions of the excited states[2,9] the computational effort to include both effects would be significant. Additionally, the symmetry of the electronic excited states has to be determined with luminescence excitation spectroscopy. This includes experiments on the dependence of the direction of the wave vector, polarization properties, and magnetic field-induced splittings. Considerable more efforts in experiment and theory are needed to achieve a more detailed picture on the symmetry and ordering of those energy levels which is clearly beyond the scope of this paper. While this can improve the agreement between theory and experiment, it will not bring new insight into the basic understanding of the nature of these excited state transitions.

We have also taken into consideration the effects caused by isotope splitting. The above-mentioned impurities B and Cl have natural abundances of ^{10}B to ^{11}B of 20:80 and ^{35}Cl to ^{37}Cl of 75:25. The influence on the binding energy was estimated to be on the order of 0.05–0.1 meV and to be a factor of three smaller for the localization energy as derived by Haynes rule.[9,11] These splittings are too small to be experimentally resolved and therefore isotope effects can be ruled out.

At present, we have found no evidence for excitons bound to acceptors (A^0X) in the investigated samples, although acceptor impurities such as Li, Na, and Cu are detected by mass spectrometry. In the investigation presented in Ref. 3 the concentration of nitrogen, a possible acceptor in ZnO, was around 5×10^{18} cm^{-3}, again without evidence for an A^0X recombination. While exciton binding to deep acceptors is not likely to occur, the absence of an excitonic line for the shallow nitrogen-related acceptor in ZnO remains a mystery, and needs further investigations.

VI. SUMMARY

In summary, we studied ground- and excited-state properties of neutral donor bound excitons in ZnO bulk crystals and

epitaxial films. We have shown that the ground and excited states can easily be distinguished on the basis of temperature-dependent luminescence and luminescence excitation experiments. In contrast to ground states, excited states of bound excitons exhibit at low temperature an intensity increase with increasing temperature. The specific activation energy of these transitions is characteristic for the different types of excited state. In particular, three groups of excited states of excitons bound to a neutral donor leaving the donor in the ground state were observed. The lowest energy separation to the ground state is found for vibrational-rotational excited states of the excitons which are placed approximately 1–2 meV above the ground state and scale with the localization energies of the bound excitons. Magneto-optical PL spectra revealed comparable electron g values of $g_e^{\perp}=1.96$ for the ground and excited states of the donor bound excitons. The next group of excited states is given by excitons which involve a hole from the B- instead of the A-valence band. These transitions are separated from each other by a (within experimental errors) constant energy spacing of 4.5 meV which makes it particularly easy to identify them. The last group involves electronic excited states of the excitons which start above the B-valence-band transitions and are considerable more complex. These excited states were studied by photoluminescence excitation spectroscopy. Based on theoretical calculations for the neutral donor bound excitons I_4 to I_9, we have presented possible assignments for all donor bound exciton excited states.

ACKNOWLEDGMENTS

Parts of this work were supported by the DFG within SFB 787. M.R.W. acknowledges support of the cluster of excellence "Unifying Concepts in Catalysis—UniCat."

*bruno.k.meyer@exp1.physik.uni-giessen.de

[1] C. Klingshirn, Phys. Status Solidi B **244**, 3027 (2007).
[2] B. K. Meyer, J. Sann, S. Lautenschläger, M. R. Wagner, and A. Hoffmann, Phys. Rev. B **76**, 184120 (2007).
[3] A. V. Rodina, M. Strassburg, M. Dworzak, U. Haboeck, A. Hoffmann, A. Zeuner, H. R. Alves, D. M. Hofmann, and B. K. Meyer, Phys. Rev. B **69**, 125206 (2004).
[4] J. Sann, Ph.D. thesis, University of Giessen, 2008.
[5] G. Blattner, C. Klingshirn, R. Helbig, and R. Meinl, Phys. Status Solidi B **107**, 105 (1981).
[6] J. Gutowski, N. Presser, and I. Broser, Phys. Rev. B **38**, 9746 (1988).
[7] M. R. Wagner, J.-H. Schulze, R. Kirste, M. Cobet, A. Hoffmann, C. Rauch, A. V. Rodina, B. K. Meyer, U. Röder, and K. Thonke, Phys. Rev. B **80**, 205203 (2009).
[8] L. Ding, B. K. Li, H. T. He, W. K. Ge, J. N. Wang, J. Q. Ning, X. M. Dai, C. C. Ling, and S. J. Xu, J. Appl. Phys. **105**, 053511 (2009).
[9] B. K. Meyer, H. Alves, D. M. Hofmann, W. Kriegseis, D. Forster, F. Bertram, J. Christen, A. Hoffmann, M. Straßburg, M. Dworzak, U. Haboeck, and A. V. Rodina, Phys. Status Solidi B **241**, 231 (2004).
[10] J. Puls, F. Henneberger, and J. Voigt, Phys. Status Solidi B **119**, 291 (1983).
[11] J. R. Haynes, Phys. Rev. Lett. **4**, 361 (1960).
[12] P. H. Kasai, Phys. Rev. **130**, 989 (1963).
[13] M. Brandt, H. von Wenckstern, G. Benndorf, M. Lange, C. P. Dietrich, C. Kranert, C. Sturm, R. Schmidt-Grund, H. Hochmuth, M. Lorenz, M. Grundmann, M. R. Wagner, M. Alic, C. Nenstiel, and A. Hoffmann, Phys. Rev. B **81**, 073306 (2010).